

Tactic direction determined by the interaction between oscillatory chemical waves and rheological deformation in an amoeba

Kei-Ichi Ueda

Department of Life, Information and System Sciences, Graduate School of Science and Engineering, University of Toyama, Toyama 930-8555, Japan

Seiji Takagi

Research Institute for Electronic Science, Hokkaido University, Sapporo 001-0020, Japan

Toshiyuki Nakagaki

Department of Complex and Intelligent Systems, Faculty of Systems Information Science, Future University Hakodate, Hakodate 041-8655, Japan and Japan Science and Technology Agency, Core Research for Evolutional Science and Technology, Chiyoda-ku, Tokyo 102-0075, Japan

(Received 28 September 2011; published 27 July 2012)

The survival of an organism can depend upon the direction in which it decides to move in response to changes in external conditions. Here we propose a physicochemical mechanism of the decision process for migration direction in the case of a giant amoebalike *Physarum* plasmodium. The tactical movement response could be changed by reversal of the phase wave of the rhythmic contractions that occur in any part of the plasmodium body when local stimulation is applied and the frequency of the rhythmic contractions is locally modulated in the stimulated region. The proposed model describes a physicochemical mechanism of coupling between the local modulation of frequency and the global transport of protoplasmic mass. The decision process is clarified from a rheological point of view.

DOI: [10.1103/PhysRevE.86.011927](https://doi.org/10.1103/PhysRevE.86.011927)

PACS number(s): 87.17.Jj, 05.40.-a, 87.17.Aa

I. INTRODUCTION

It is crucial for organisms to decide the best direction in which to move in response to changes in external conditions. The physiological roles and purpose of this decision process have been discussed previously, but the process remains unclear in terms of the equation of motion that is derived from physical and chemical considerations of cellular movement. The amoebalike plasmodium of the slime mold *Physarum* has been recognized as a useful model organism in which to study questions of this kind [1–3].

Rhythmic contraction of the mechanochemical system is obvious throughout the *Physarum* body, and various types of pattern and wave are formed in response to stimulation. Matsumoto and co-workers proved experimentally that modulation of phase waves played a key role in deciding the direction of migration. Their experiment was roughly based on the entrainment of cellular rhythms, including Ca^{2+} and adenosine triphosphate (ATP) oscillation, and contraction-relaxation cycles [4,5]. Regardless of the physical nature of the stimuli (light, temperature, or chemical), the cellular rhythms were slowed down or accelerated locally in the affected parts of the body in response to attractive or repulsive stimulation, respectively. As studied in Ref. [6], slight spatially modulation of the rhythmicity led to wave propagation of the phase of oscillation. Matsumoto and co-workers showed that the direction of phase wave propagation was opposite the direction of the tactical migration response. This finding provided elegant evidence that the collective behavior of biochemical oscillators plays an important role in information processing in living systems [1]. The present paper clarifies the dynamic mechanism of the observed phenomenon.

It has been reported that chemical concentration patterns are used as tactical signals in a variety of cellular organisms [7–13]. Cellular biochemical processes, such as rhythmic actomyosin contraction, sol-gel transformation, and tip formation for migration, are not independent, but rather are closely related to each other. Recently, pattern formation of chemical waves driven by active fluids has been extensively studied [14,15].

In *Physarum*, by integrating these processes, the net transport of the protoplasmic mass as a tactical response is possible. Dilution from sol streaming, generated by the phase difference of the chemical oscillators, has been reported to affect the rhythmic contraction patterns in *Physarum* [16,17]. However, the mechanism of the rheological deformation (thickness change of the organism) driven by the frequency difference of the chemical oscillators is unclear. Several pioneering works concerning cytoplasmic rhythm and streaming have been reported [18–20]. Building upon these studies, the present work aims to shed light on the interplay of chemical oscillations and rheological deformation.

II. MODEL

The locomotion of *Physarum* is accomplished through the following steps. (i) In order to generate a leading edge, the organism decreases the stiffness of the gel at the boundary edge by means of chemical reactions that occur there. At this stage, the Ca^{2+} concentration, which is believed to be one of the solation factors, increases at the boundary edge. As the stiffness of the gel at the front part of the plasmodium decreases, the pressure of the sol that part

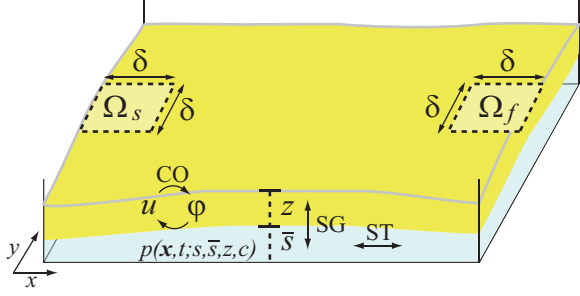


FIG. 1. (Color online) Schematic illustration of the setup of our numerical experiments. The thicknesses of the gel and sol layers are z and \bar{s} , respectively. The thickness of the gel changes with time due to sol-gel transformation (SG). The shuttle streaming of the sol (ST) is generated by the pressure gradient. The chemical oscillation (CO) is generated by c and φ . The pressure of the sol is a function of s , \bar{s} , z , and c . The term Ω_s is a stimulated site, where τ is taken as a control parameter, and Ω_f is a free site, which serves as a reference.

decreases concomitantly. (ii) The sol is transported from the rear part to the leading edge by the pressure gradient generated in step (i). (iii) When the thickness of the sol exceeds a threshold level, the organism begins to migrate.

In light of step (i), the Ca^{2+} concentration is a critical factor in deciding the direction that the organism migrates. In this article we focus on steps (i) and (ii). In particular, we investigate how the frequency of the chemical oscillation controls the concentration of Ca^{2+} .

Our model is based on that reported previously in Refs. [19,21] and is illustrated in Fig. 1. Our model system comprises two parts: an outer gel composed of actomyosin filaments surrounding an inner flowing sol. The streaming of the protoplasmic sol is driven by a pressure gradient generated by contraction of the actomyosin filaments in the gel. The equations for the dynamics of the sol and gel are the same as those derived in Ref. [21]:

$$s_t = \nabla \cdot (sM\nabla p) + \gamma(z - s), \quad (1)$$

$$z_t = D_z \nabla^2 z + \gamma(s - z), \quad (2)$$

$$\mathbf{x} = (x, y) \in [0, 1] \times [0, 1], \quad t > 0,$$

where $\nabla = (\partial/\partial x, \partial/\partial y)$; $s(\mathbf{x}, t)$ is the thickness (or density) of the sol; $z(\mathbf{x}, t)$ is the thickness of the gel; and M , γ , and D_z are coefficients. The sol flows according to Darcy's law and its conversion to the gel is described by $\gamma(z - s)$, which reduces the contrast with the gel thickness. The gel diffuses slowly and its conversion to the sol is described by $\gamma(s - z)$. The total mass of the organism ($s + z$) is conserved over the entire space.

The basal thickness of the sol for the organism is described by $s_b(\mathbf{x}, t)$, which is the volume capacity of the cavity bounded by the gel cortex. We assume that the basal thickness acts like the natural length of a Hookean spring and thus the elastic force is governed by the displacement of contraction from the basal thickness s_b . Thus the pressure of the sol is governed by $p = \beta(s - s_b)$.

The basal thickness s_b varies periodically in time due to the actomyosin contraction. The periodic contraction is generated by periodic variations of chemical concentration. It has been

experimentally observed that the contraction takes place at low concentrations of Ca^{2+} oscillation [5]. In addition, the amplitude of the contraction increases as the thickness of the gel (z) increases. Thus we assume that the dynamics of $s_b(\mathbf{x}, t)$ are described as follows:

$$s_b = \bar{s} + az(c - \bar{c}), \quad (3)$$

where $c = c(\mathbf{x}, t)$ is the concentration of Ca^{2+} , $\bar{s}(\mathbf{x}, t)$ is the mean thickness of the sol layer, and a and \bar{c} are constants. The time-averaged thickness \bar{s} is described by $\bar{s}_t = \gamma_s(s - \bar{s})$, where γ_s is a constant.

Equations (1) and (2) indicate that z increases with time due to the sol-gel transformation. Therefore, the tactical responses shown in the experiments might be established by disrupting the balance between the inflow and outflow rates of the sol in the stimulated area. Our hypothesis is that the modulation of the chemical oscillator (the actomyosin contraction) by the accumulation of the sol (rheological deformation of the organism) plays an important role in disrupting this balance. This hypothesis is based on the finding that the presence of the interaction between the chemical period and the amplitude of contraction oscillation is modulated locally at the place where the sol gathers and scatters [22].

In Refs. [19,21] actomyosin contraction generated by chemical oscillations of Ca^{2+} , ATP, and so on was simply described by $\sin(\omega t)$, which is the independent function of \mathbf{x} . Here we employ a more realistic model equation, namely, the Smith-Saldana (SS) model [23,24], based on a biochemical analysis of the time period of Ca^{2+} fluctuations. We include the diffusion of Ca^{2+} in the gel layer and the chemical oscillator is assumed to be affected by the amount of sol as follows:

$$c_t = f(c, \varphi)/\tau + \kappa_1 s + D_c \Delta c, \quad \varphi_t = g(c, \varphi)/\tau + \kappa_2 s, \quad (4)$$

where $\Delta = \partial^2/\partial x^2 + \partial^2/\partial y^2$, $c(\mathbf{x}, t)$ is the concentration of Ca^{2+} , $\varphi(\mathbf{x}, t)$ is the probability of a myosin light-chain kinase being phosphorylated, $f(c, \varphi) = -k_V n_c(c, \varphi) + k_L(N_c - c)$, and $g(c, \varphi) = K_Q(n_c(c, \varphi))(1 - \varphi) - k_E \varphi$, with $K_Q(n_c) = k_Q\{K_* n_c(c, \varphi)/[1 + K_* n_c(c, \varphi)]\}$ and $n_c(c, \varphi) = [1 + 0.17(c - 7.5)](a_0 + a_1 \varphi + a_2 \varphi^2 + a_3 \varphi^3)$. The same parameter values as those in Ref. [24] are set: $a_0 = 0.349353$, $a_1 = -0.0454567$, $a_2 = 1.15905$, $a_3 = 1.823858$, $k_V = 0.12$, $k_L = 0.004$, $k_Q = 1.0$, $k_E = 0.1$, $K_* = 1.75$, and $N_c = 25.0$. The first terms of the c and φ equations generate a limit cycle and κ_1 and κ_2 are the coupling coefficients between the amount of the sol and the chemical oscillator. A weak coupling is assumed such that the values of $|\kappa_j|$ are small. Equation (4) is used for actomyosin contraction unless otherwise stated.

The length of the plasmodium and the period of oscillation are nondimensionalized by the characteristic length and period of actomyosin contraction in a fashion similar to that reported in Ref. [19]. The pressure p and stiffness β are nondimensionalized by the typical pressure estimated at approximately $1.5 \times 10^4 \text{ N/m}^2$. The parameters are set as $a = 0.1$, $\beta = 20.0$, $\gamma_s = 10.0$, $D_c = 2.0 \times 10^{-3}$, $D_z = 0.01$, and $\bar{c} = 8.7$. The Neumann boundary condition is imposed. The time increment is $\Delta t = 0.1$ and the grid size is 50×50 .

The experiments conducted by Matsumoto *et al.* [1] showed that the tactical response could be controlled by the local modulation of the frequency of actomyosin contractions; specifically, the organism was attracted to and repelled from

the positions where the frequency was higher and lower, respectively. In numerical simulations, the frequency could be controlled by changing τ in Eq. (4). Thus the frequency control is represented by taking τ as a function of space variables:

$$\tau(\mathbf{x}) = \begin{cases} \tau_0 r_s, & \mathbf{x} \in \Omega_s, t \geq t_p \\ \tau_0, & \text{otherwise,} \end{cases} \quad (5)$$

where $\tau_0 = 0.1$, Ω_s is the position where the frequency is controlled, and t_p is the time when perturbation is first applied. We set $t_p = 2.0$ and $\Omega_s : (x, y) \in [0, \delta] \times [(1 - \delta)/2, (1 + \delta)/2]$, where $\delta = 0.2$. As τ corresponds to the time constant of the kinetics part of Eq. (4), a small r_s means a high frequency at Ω_s . For convenience, we refer to Ω_s as the stimulated site (*S* site) and define the free site (*F* site) $\Omega_f : (x, y) \in [1 - \delta, 1] \times [(1 - \delta)/2, (1 + \delta)/2]$ as a reference (Fig. 1).

III. RESULTS

We now consider how the interaction between the chemical oscillator and the sol amount affects the migration direction. Periodic change in the thickness of the organism due to periodic shuttle streaming is observed when $r_s \neq 1$, irrespective of whether the interaction is absent or present. When $r_s < 1$ ($r_s > 1$), the phase of the contraction is advanced (delayed) and the amplitude of the thickness oscillation at the *S* site becomes larger than that at the *F* site [Figs. 2(a)–2(d)]. In response to the change in frequency of the contraction, the time-averaged thickness of the organism (or the amount of the sol) either decreases or increases depending on κ_1 and κ_2 .

By taking κ_1 and κ_2 as control parameters, the balance between the inflow and outflow rates of the amount of the

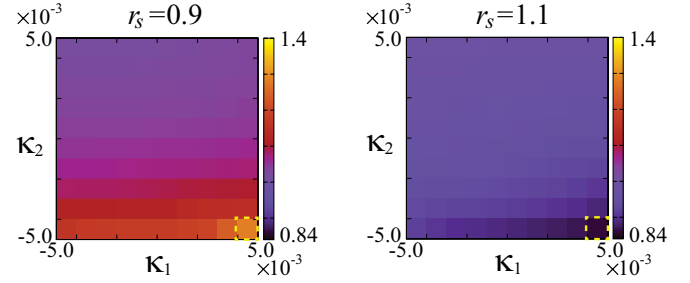


FIG. 3. (Color online) Tactical response depending on κ_j for the SS model with $r_s = 0.9$ (left) and $r_s = 1.1$ (right). The time-averaged thickness Z_8 is displayed. The thickness attained a maximum for $r_s = 0.9$ and a minimum for $r_s = 1.1$ at $(\kappa_1, \kappa_2) = (0.005, -0.005)$.

sol at the *S* site can be changed. Figure 3 shows a phase diagram of the time-averaged thickness at the *S* site, where the time-averaged thickness is defined as $Z_i = \int_{t_i}^{t_i+1} z dt / T$ and t_i denotes the time when u attains the local maximum. The parameters κ_1 and κ_2 are changed in the region $(\kappa_1, \kappa_2) \in [-0.005, 0.005] \times [-0.005, 0.005]$. The changes in (κ_1, κ_2) from the top left-hand corner to the bottom right-hand corner in the diagram with $r_s = 0.9$ and $r_s = 1.1$ cause gradual increases and decreases, respectively, in the averaged thickness Z_8 [Fig. 3]. For both cases, $r_s = 0.9$ and 1.1 , Z_8 show relatively few changes when the interaction between the chemical oscillator and the sol is absent, that is, $(\kappa_1, \kappa_2) = (0, 0)$. These numerical results indicate the following: (i) The interaction is crucial to break the balance of the sol flow rates at the *S* site and (ii) the actual responses observed by Matsumoto

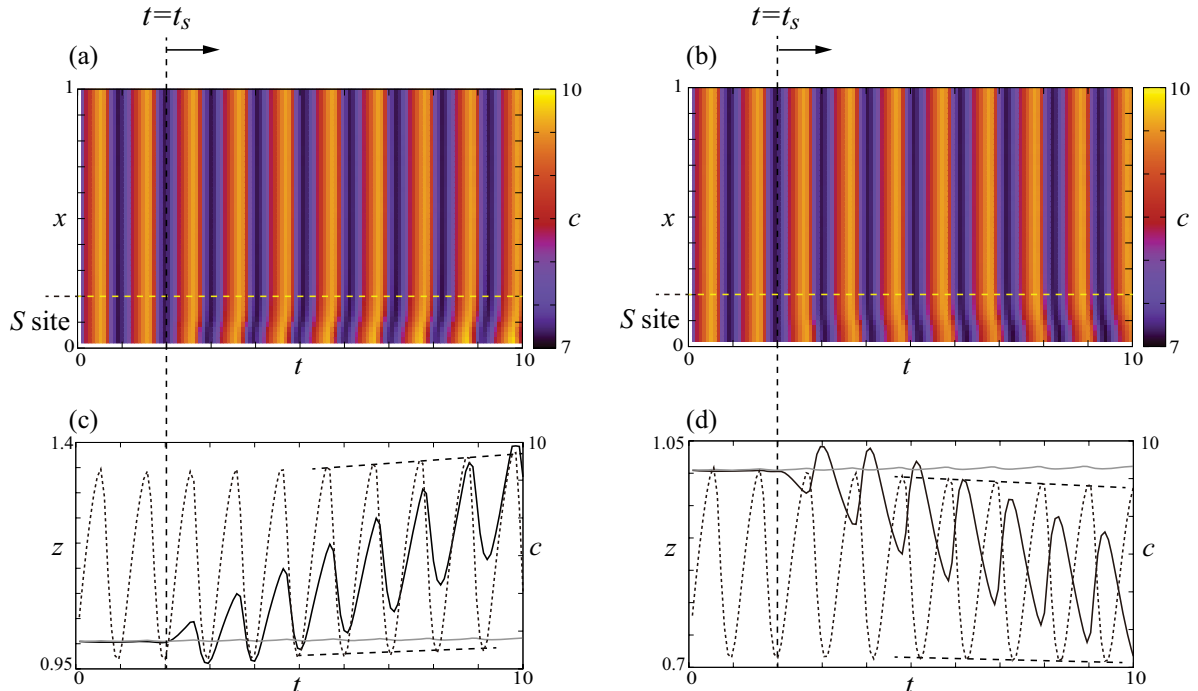


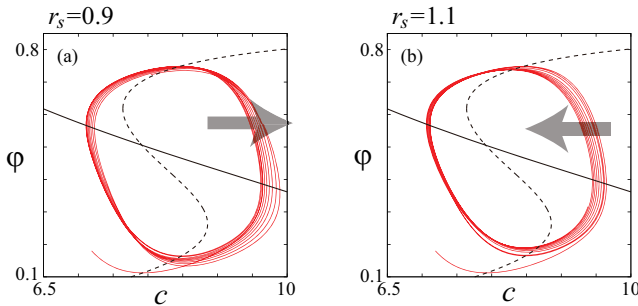
FIG. 2. (Color online) Tactical response for the Smith-Saldana model. Solutions are shown for (a) and (c) $r_s = 0.9$ and (b) and (d) $r_s = 1.1$, with $(\kappa_1, \kappa_2) = (0.005, -0.005)$. (a) and (b) Time series of the Ca^{2+} concentration for $y = 1/2$. (c) and (d) Black and gray lines indicate z at the *S* and *F* sites, respectively. Dotted lines indicate c at the *S* site.

et al. [1] are reproduced when κ_1 and κ_2 are taken from the bottom right-hand corner in the diagram. Hereinafter, we assume $(\kappa_1, \kappa_2) = (0.005, -0.005)$ in order to investigate the mechanism.

As shown in the experiments [1], the baseline of z at the S site increases and decreases as the phase of the chemical oscillator is advanced and delayed, respectively [dashed lines in Figs. 2(c) and 2(d); see also Figs. 4(a) and 4(b)]. In addition, the baseline of c also increases and decreases for $t > t_s$ when $r_s = 0.9$ and 1.1, respectively. Such responses of c are crucial for the change in Z_i . According to the p and s_b equations, s increases (decreases) as the time-averaged value of c over the unit time interval increases (decreases), suggesting that z increases (decreases) through the sol-gel conversion [see Eqs. (1) and (2)]. We should therefore consider the mechanism by which the baseline of c increases and decreases through the interaction of the dynamics of the sol for $r_s < 1$ and $r_s > 1$, respectively.

The influence of the interaction on the dynamics of c can be clearly shown by drawing the solution orbit of c and φ . In the presence of the interaction, the position of the circle of c in the phase plane moves to the right for $r_s = 0.9$ [gray arrows in Fig. 4(a)]. As a result, the baseline of c increases as the time increases. By contrast, the position of the circle of c moves to the left for $r_s = 1.1$ and the baseline of c at the S site decreases [gray arrows in Fig. 4(b)]. Thus we can find

Smith-Saldana model



Stuart-Landau model

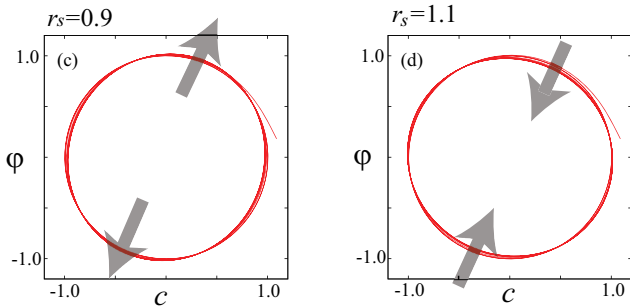


FIG. 4. (Color online) Solution orbits of (a) and (b) the SS model and (c) and (d) the SL model in the c - φ plane at the S site. (a) $r_s = 0.9$ and $(\kappa_1, \kappa_2) = (0.005, -0.005)$ and (b) $r_s = 1.1$ and $(\kappa_1, \kappa_2) = (0.005, -0.005)$. The black solid and dashed lines indicate the null cline of c and φ with $(\kappa_1, \kappa_2) = (0, 0)$. The solution orbits move to the directions indicated by gray arrows. (c) $r_s = 0.9$ and $(\kappa_1, \kappa_2) = (0.005, -0.005)$ and (d) $r_s = 1.1$ and $(\kappa_1, \kappa_2) = (0.005, -0.005)$.

resonance between the periodic oscillation of (c, φ) and the rhythmic sol flow, generated by the spatial graduation of the phase of the actomyosin contraction around the S site.

It should be noted that the periodic motion of (c, φ) and the interaction of the sol are not sufficient to account for the tactical responses. One representative model showing periodic oscillations is the Stuart-Landau (SL) equation, which was used in Refs. [19,25]: $f(c, \varphi) = c - \varphi - c(c^2 + \varphi^2)$ and $g(c, \varphi) = c + \varphi - \varphi(c^2 + \varphi^2)$. We now compare the dynamics of the SS model and the SL equation. To ensure that the experimental conditions (such as the oscillation frequency and the minimum and maximum p) are as similar as possible to those of the SS model, the parameters τ , a , and \bar{c} are set for the SL system such that $\tau_0 = 0.2336$, $a = 0.111$, and $\bar{c} = 0.70$ and the parameters κ_1 and κ_2 are changed in the region $(\kappa_1, \kappa_2) \in [-0.005, 0.005] \times [-0.005, 0.005]$.

It was found that Z_8 increases as the frequency of the S site increases for $r_s \in [0.9, 1.1]$. However, the difference in Z_8 between $r_s = 0.9$ and 1.1 is much smaller than that for the SS model ($Z_8 = 1.06$ for $r_s = 0.9$ and $Z_8 = 0.96$ for $r_s = 1.1$) because the resonance does not occur; the increasing and decreasing rates of the thickness saturate quickly in comparison with the SS model (Fig. 5). These numerical results do not capture the actual observation.

The solution orbit of the SL equation in the c - φ plane for $(\kappa_1, \kappa_2) = (0.005, -0.005)$ is shown in Figs. 4(c) and 4(d). For $r_s = 0.9$ ($r_s = 1.1$), the shape of the limit cycles becomes elliptical; the top right-hand corner and the bottom left-hand corner expand (shrink) in the direction of the arrows as shown in Figs. 4(c) and 4(d), where $(\kappa_1, \kappa_2) = (0.005, -0.005)$ for $r_s = 0.9$ and 1.1, respectively. However, in contrast to the case of SS, the position of the rotating center shows negligible changes, as does the mean thickness. This suggests that the resonance, which can change the position of the rotating center of c , is required for the mechanism.

IV. DISCUSSION

The effect of the interaction between the fluid and chemical reactions has been studied, for example, in Refs. [15,16]. In the case of *Physarum*, the numerical results in Fig. 5 suggested that the existence of the interaction is not a sufficient condition to reproduce the actual observation shown by Matsumoto *et al.* [1]. The mathematical model presented here showed that the Ca^{2+} concentration change due to the resonance through the interaction between the rhythmic streaming of the sol and the chemical oscillators is a key mechanism for tactical responses. We remark that such a cooperative response between z and c has also been observed experimentally [26].

Stich and Mikhailov have studied the dispersion relation of the complex Ginzburg-Landau (GL) equation [6]:

$$\begin{aligned} u_t &= \nabla^2(u - \tilde{\beta}v) + (u + \tilde{\omega}v) - (u - \tilde{\alpha}v)(u^2 + v^2), \\ v_t &= \nabla^2(\tilde{\beta}u + v) + (-\tilde{\omega}u + v) - (\tilde{\alpha}u + v)(u^2 + v^2), \end{aligned} \quad (6)$$

where $\tilde{\omega}(x, y) \equiv \Omega + \delta\omega(x, y)$ and Ω is a constant. The heterogeneity function $\delta\omega(x, y)$ is defined as follows:

$$\delta\omega(x, y) = \begin{cases} \Delta\omega, & \mathbf{x} \in \Omega_s \\ 0, & \text{otherwise.} \end{cases} \quad (7)$$

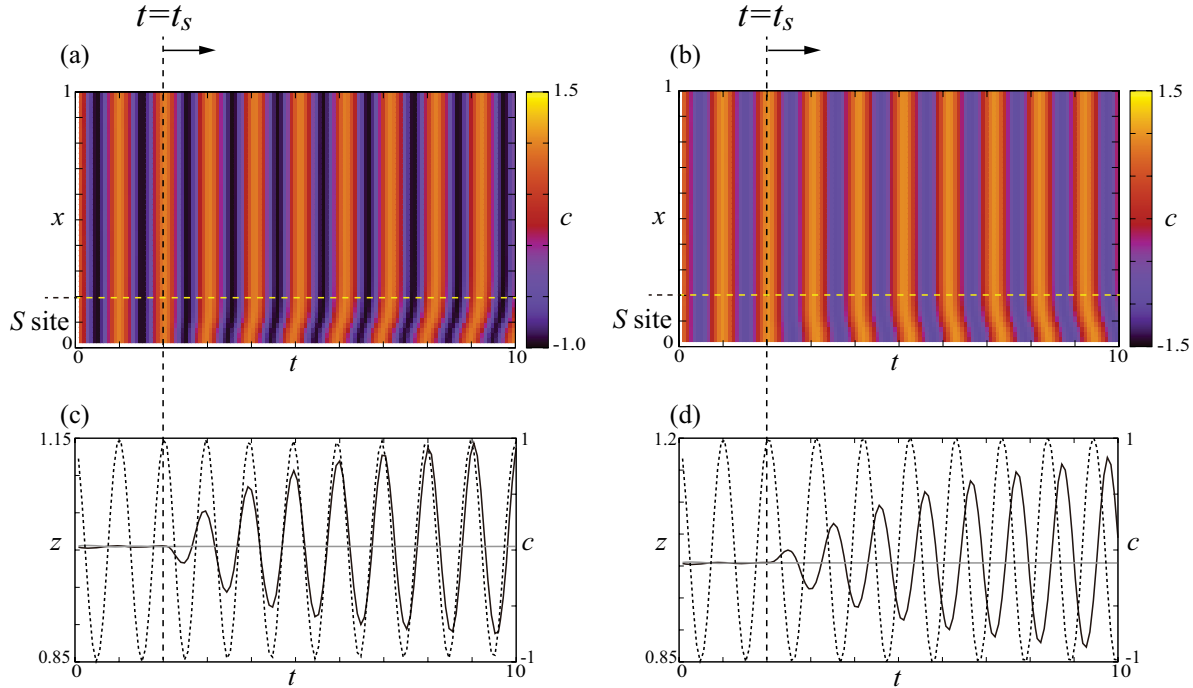


FIG. 5. (Color online) Tactical response for the Stuart-Landau model. Solutions are shown for (a) and (c) $r_s = 0.9$ and (b) and (d) $r_s = 1.1$, with $(\kappa_1, \kappa_2) = (0.005, -0.005)$. (a) and (b) Time series of the Ca^{2+} concentration for $y = 1/2$. (c) and (d) Black and gray lines indicate z at the S and F sites, respectively. Dotted lines indicate c at the S site.

From their results, heterogeneity of the oscillation frequency acts as wave source [sink] when $(\tilde{\beta} - \tilde{\alpha})\Delta\omega > 0$ [$(\tilde{\beta} - \tilde{\alpha})\Delta\omega < 0$]. We use Eq. (6) to describe the chemical oscillator; in other words, Eq. (4) is replaced as follows:

$$\begin{aligned} c_t &= \nabla^2(c - \tilde{\beta}\varphi) + f(c, \varphi)/\tau + \kappa_1 s, \\ \varphi_t &= \nabla^2(\tilde{\beta}c + \varphi) + g(c, \varphi)/\tau + \kappa_2 s, \end{aligned} \quad (8)$$

where $f(c, \varphi) = (c + \tilde{\omega}\varphi) - (c - \tilde{\alpha}\varphi)(c^2 + \varphi^2)$ and $g(c, \varphi) = (-\tilde{\omega}c + \varphi) - (\tilde{\alpha}c + \varphi)(c^2 + \varphi^2)$. Positive (negative) dispersion corresponds to $\tilde{\beta} - \tilde{\alpha} > 0$ ($\tilde{\beta} - \tilde{\alpha} < 0$). We conducted numerical simulations by taking $(\tilde{\alpha}, \tilde{\beta}) = (-1, 0)$ (positive dispersion) with $(\kappa_1, \kappa_2) = (0.005, -0.005)$ and we found that the thickness of the organism decreases [increases] when the frequency of the oscillation is higher ($\Delta\omega > 0$) [lower ($\Delta\omega < 0$)] at the stimulated site. In addition, in the case of negative dispersion, the opposite situation arises; that is, the thickness of the organism increases when $\Delta\omega > 0$ and vice versa. It follows from these results that the wave propagation direction is crucial for the tactical responses. However, we could not find the resonance; that is, we could

not succeed in reproducing the actual observation for the GL equation.

Lastly, we make a comparison with the motor control of higher animals. The central nervous system processes information, the motile organs move the body, and the former controls the latter. This parallels the tactical movement response observed in *Physarum*. In this organism, chemical oscillators can be regarded as the information processing system that controls the organs of motility. From this point of view, the current work proposes a dynamic mechanism for coordinating the body and information processing system in *Physarum*, which might represent a primitive mechanism of locomotion control in animals.

ACKNOWLEDGMENTS

This work was supported by Grants-in-Aid for Scientific Research (No. 20300105 and No. 22740064), the Strategic Japanese-Swedish Research Cooperative Program, and the Japan Science and Technology Agency. We thank Ryo Kobayashi for useful comments.

-
- [1] K. Matsumoto, T. Ueda, and Y. Kobatake, *J. Theor. Biol.* **131**, 175 (1988).
 [2] Y. Mori, K. Matsumoto, T. Ueda, and Y. Kobatake, *Protoplasma* **135**, 31 (1986).
 [3] T. Ueda, K. Matsumoto, T. Akitaya, and Y. Kobatake, *Exp. Cell Res.* **162**, 486 (1986).

- [4] Y. Yoshimoto, T. Sasaki, and N. Kamiya, *Protoplasma* **109**, 159 (1981).
 [5] Y. Yoshimoto, F. Matsumura, and N. Kamiya, *Cell Motil.* **1**, 433 (1981).
 [6] M. Stich and A. S. Mikhailov, *Physica D* **215**, 38 (2006).

- [7] R. J. Petrie, A. D. Doyle, and K. M. Yamada, *Nat. Rev. Mol. Cell Biol.* **10**, 538 (2009).
- [8] C. Wei, X. Wang, M. Chen, K. Ouyang, L.-S. Song, and H. Cheng, *Nature (London)* **457**, 901 (2009).
- [9] Y. Arai, T. Shibata, S. Matsuoka, M. J. Sato, T. Yanagida, and M. Ueda, *Proc. Natl. Acad. Sci. USA* **107**, 12399 (2010).
- [10] K. Dubrovinski and K. Kruse, *Phys. Rev. Lett.* **107**, 258103 (2011).
- [11] G. Gerisch, M. Ecke, B. Schroth-Diez, S. Gerwig, U. Engel, L. Madder, and M. Clarke, *Cell Adh. Migr.* **3**(4), 373 (2009).
- [12] Y. Asano, A. Nagasaki, and T. Q. P. Uyeda, *Cell Motil. Cytoskel.* **65**, 923 (2008).
- [13] K. J. Tomchik and P. N. Devreotes, *Science* **212**, 443 (1981).
- [14] J. Howard, S. W. Grill, and J. S. Bois, *Nat. Rev. Mol. Cell Biol.* **12**, 392 (2011).
- [15] J. S. Bois, F. Jülicher, and S. W. Grill, *Phys. Rev. Lett.* **106**, 028103 (2011).
- [16] M. Radszweit, H. Engel, and M. Bär, *Eur. Phys. J. Spec. Top.* **191**, 159 (2010).
- [17] H. Yamada, T. Nakagaki, R. E. Baker, and P. K. Maini, *J. Math. Biol.* **54**, 745 (2007).
- [18] V. A. Teplov, Yu. M. Romanovsky, and O. A. Latushkin, *BioSystems* **24**, 269 (1991).
- [19] R. Kobayashi, A. Tero, and T. Nakagaki, *J. Math. Biol.* **53**, 273 (2006).
- [20] S. Takagi and T. Ueda, *Physica D* **237**, 420 (2008).
- [21] K.-I. Ueda, S. Takagi, Y. Nishiura, and T. Nakagaki, *Phys. Rev. E* **83**, 021916 (2011).
- [22] N. Kamiya and T. Tanaka, *Proc. Jpn. Acad.* **43**, 537 (1967).
- [23] D. A. Smith and R. Saldana, *Biophys. J.* **61**, 368 (1992).
- [24] D. A. Smith, *Protoplasma* **177**, 171 (1994).
- [25] A. Tero, R. Kobayashi, and T. Nakagaki, *Physica D* **205**, 125 (2005).
- [26] K. Natsume, Y. Miyake, M. Yano, and H. Shimizu, *Cell Struct. Funct.* **18**, 111 (1993).